scientific reports

OPEN

Investigating tectonic links between the deep Volturno plain and Campanian volcanism using vintage seismic and potential field data

Pier Paolo G. Bruno[1,2]✉, Maria Luisa Putignano[3], Federico Cella[4] & Giovanni Florio[1]

This study investigates the tectonic and subsurface structure of the Volturno Plain, a region linking the Southern Apennines with active volcanic districts of Campania. Vintage seismic profiles were vectorized, depth-converted, and integrated with historical gravity and magnetic data. The analysis reveals a coastal half-graben structure primarily controlled by NE-trending normal faults, with NW-trending faults that downthrow the carbonate outcrops of the Southern Apennines toward the coast. These fault systems collectively drive subsidence exceeding 5 km beneath the mouth of the Volturno River. Enhanced Horizontal Derivative analysis of gravity data extends fault traces beyond the seismic coverage and helps to characterize major NE-striking fault systems, such as the Mt. Massico and Villa Literno fault zones, which are likely active and exhibit aseismic creep or low-magnitude seismicity. Gravity and magnetic anomalies highlight variations in the thickness of the sedimentary cover within fault-controlled depressions, as well as the presence of volcanic deposits in the southern plain, associated with buried volcanic edifices whose emplacement was influenced by NE- and NW-trending faults. InSAR-derived surface deformation patterns show a partial alignment with these fault systems but also reflect non-tectonic factors such as sediment compaction and anthropogenic activities. Our findings confirm the structural control of NE-trending faults on the plain's evolution and Campanian volcanism. This work fills a knowledge gap regarding the tectonic and structural setting of the carbonate basement in the northern part of the Campanian Plain, for which a map of the depth to the base of the post-Miocene sedimentary cover was not yet available. This paper also highlights the value of integrating legacy seismic and potential field data using modern techniques to unravel the interplay of tectonic and magmatic processes.

The Volturno River Plain, located to the north of the Campanian Plain, is a vast alluvial plain bordered to the north by the Roccamonfina volcanic complex[1,2] and Mt. Massico[3], to the northeast by the Caserta Mountains[4], and to the south by the Campi Flegrei volcanic system[5]. The Volturno Plain formation is linked to the subsidence of the Tyrrhenian margin of the Apennine chain, occurred during the middle and lower Pleistocene[6–8] along NW-SE and NE-SW trending regional faults that displaced Meso-Cenozoic carbonatic rocks, sinking them down towards the Tyrrhenian margin. Tectonic subsidence brought the Mesozoic-Cenozoic Apennine units to great depths, leading to a substantial accumulation of Quaternary sediments of marine, volcanic and continental origin, reaching thicknesses, estimated to be of at least 3000 m in some areas of the plain[9,10]. This subsidence in the area began in the early Pleistocene and caused the submersion of significant portions of the Campanian Plain, as indicated by the discovery of early Pleistocene marine sediments atop Mesozoic or Miocene rocks in deep wells[10–14].

The Mesozoic-Cenozoic carbonates, submerged in the Volturno Plain, are exposed to the north and east of the study area. Carbonate rocks outcrop at Mt. Massico (Fig. 1), which delimits the graben to the NW. The relief is characterized by a basal complex consisting of dolomites, formed from the Upper Triassic to the Upper

[1]Dipartimento di Scienze della Terra, Ambiente e Risorse, Università degli Studi di Napoli "Federico II", Naples, Italy. [2]Istituto Nazionale di Geofisica e Vulcanologia, Sezione Roma 2, Roma, Italy. [3]Istituto di Geologia Ambientale e Geoingegneria, Consiglio Nazionale delle Ricerche, Roma, Italy. [4]Scuola di Scienze e Tecnologie - Sezione di Geologia, Università di Camerino, Camerino, Italy. ✉email: pierpaolo.bruno@unina.it

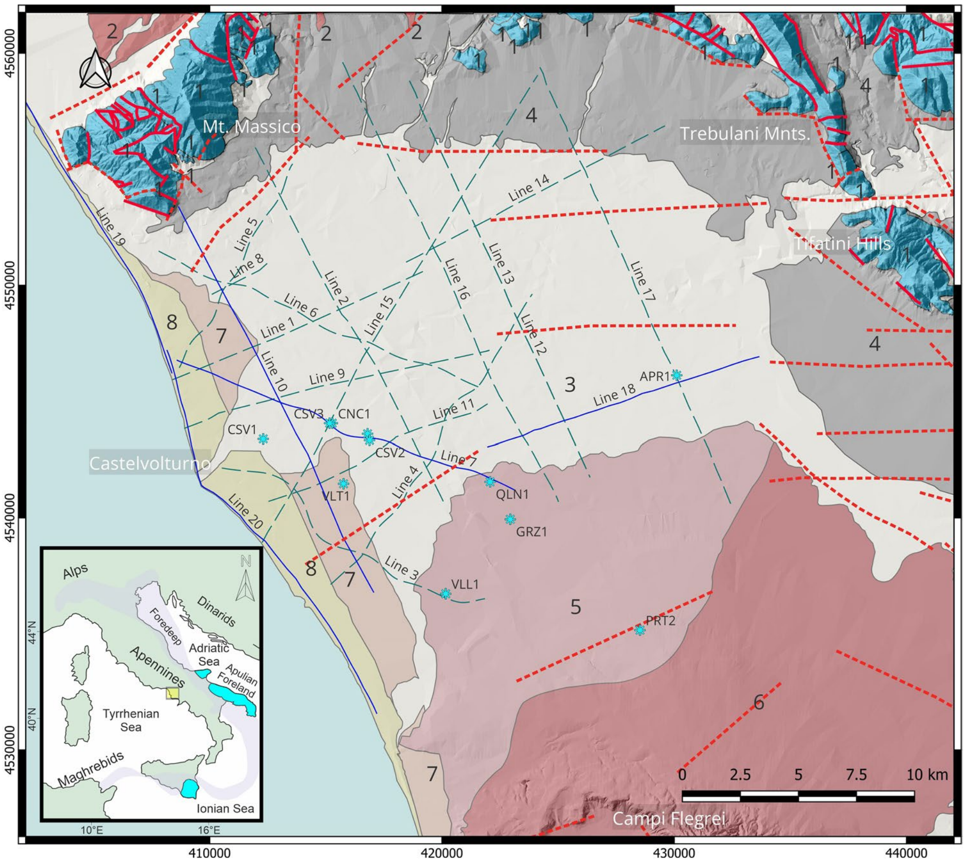

Fig. 1. Simplified geological map of the Volturno Plain. Geological Units are simplified and digitized from the maps of Vitale and Ciarcia[20] and Corrado et al.[35] and superimposed on a shadow relief of from DEM data[49], showing: (1) Meso-Cenozoic carbonatic and flysch bedrock, see details in Vitale and Ciarcia (2018); (2) Late Pleistocene-Holocene Roccamonfina reworked pyroclastites; (3) Late Pleistocene-Holocene alluvial deposits; (4) Holocene Campi Flegrei Campanian Ignimbrite deposits; (5) Holocene Campi Flegrei Neapolitan Yellow Tuff deposits; (6) Holocene Campi Flegrei fallout deposits (7) Holocene marsh deposits; (8) Holocene dunal ridge deposits. Faults, from Vitale and Ciarcia (2018), are shown in red (dashed where inferred). Symbols: dashed black lines indicate seismic profiles, with those shown in Figs. 3, 4, 5 and 6 highlighted in blue to facilitate their recognition. Asterisks in cyan color highlight the position of the exploration wells. This map was generated with QGIS (https://qgis.org/), version 3.34.11 (Prizren).

Cretaceous and cropping out along the northern front of the massif[15]. Bruno et al.[16] interpreted the NE-trending Massico Fault as the southern tip of the Ortona–Roccamonfina lineament. Seismic swarms suggest that some segments of the Ortona–Roccamonfina line remain active[17]. A listric geometry for the fault along the southern margin of Mt. Massico was proposed by Mariani & Prato[18] and Torrente & Milia[19], based on seismic reflection data and sedimentary infill growth patterns in the Campanian Plain. The horizontal displacement of Mt. Massico offshore suggests a left-lateral movement along this fault[16]. Carbonate outcrops are also found in the Caserta Mountains to the east (Fig. 1). These outcrops constitute a complex of mountain massifs, i.e., the Trebulani Mountains[20] and the Tifatini Mountains[21,22], often characterized by fractured and karstified limestone lithologies.

Since the Middle Pleistocene, the filling of the Volturno depression has been influenced not only by the interaction between fluvial inputs of Apennine origin and marine contributions but also by volcanic activity from numerous eruptive centers associated with the volcanic districts of Campi Flegrei, Somma-Vesuvius, and Roccamonfina. This volcanism developed along major structural lineaments located both at the edges and within the plain[9,11,23–25] and represents a regional feature. Volcanic activity in the region began during the Middle Pleistocene at the Roccamonfina volcanic district, which was active between 630 and 53 ka[26,27]. This activity was primarily aligned along structural axes trending NE-SW and N-S. Subsequently, volcanic activity initiated at Ischia[28] and Campi Flegrei[29] during the early late Pleistocene. Campi Flegrei are located on a structural high[30], flanked by adjacent structural lows represented by the Gulf of Naples and the Volturno Plain. This horst structure extends onto the mainland with an anti-Apennine (i.e., NE) orientation, reaching the northernmost areas of the Campanian Plain in the Caserta region[30,31]. The origin of Campi Flegrei can be traced back to two significant collapses that occurred along NE and NW structural trends and are associated with two super-eruptions: the Campanian Ignimbrite (39.8 ka, Giaccio et al.[32]) and the Neapolitan Yellow Tuff (15 ka, Deino et al.[33]). Shortly thereafter, volcanic activity began at Somma-Vesuvius[14].

Santangelo et al.[10] reconstructed the Quaternary evolution of the Volturno Plain by integrating stratigraphic and geomorphological data. Their study indicates that the region experienced significant subsidence throughout the Middle and Late Pleistocene, with volcaniclastics playing a key role in its recent evolution through extensive aggradation. During the early Middle Pleistocene, the coastline was situated further inland, at the base of the main carbonate massifs bordering the basin. Subsidence rates varied across the plain, and recent data suggest that over the past 130 ka, phases of relative tectonic stability alternated with periods of increased subsidence, particularly following major volcanic events.

Vertical displacement values obtained by the processing of interferometric data[34] show that presently Volturno river plain is characterized by significant subsidence in the central axial sectors and in the river mouth area. Moderate uplift, related to tectonic activity, characterizes the eastern part. Matano et al.[34] interpret the subsidence recorded in the Volturno Plain as being mainly a consequence of a natural process related to the compaction of the fluvial and palustrine deposits. However, it is reasonable to hypothesize that part of this subsidence might have a tectonic drive. Corrado et al.[35], based on the analysis of borehole logs and new geomorphological surveys, estimated an average tectonic subsidence rate of about 0.5 mm/year for the plain. However, the stress field acting in the whole Campanian area is poorly known. Structural observations on Pleistocene faults indicate normal-to-sinistral motion along NW-trending faults and normal-to-dextral motion along NE-trending structures[36], consistent with fault patterns along the inner margin of the Southern Apennines. Despite the high subsidence rate, the Volturno Plain exhibits significantly lower seismicity than the adjacent Apennine chain (Mw ≤ 4.8; Luiso et al.[37]). Minor seismicity (Mw < 5.5), including swarms and moderate-energy earthquakes, primarily occurs along the plain's margins, particularly in volcanic areas.

This work aims to investigate the tectonic settings in the Volturno Plain by estimating the depths and morphology of the buried carbonate basement and mapping the major fault systems that displace it. These analyses are based on seismic reflection profiles acquired in the 1970–80 s, integrated with gravity and magnetic data. Understanding the depth and structure of the carbonate basement is crucial not only for interpreting the tectonic dynamics of the area and identifying the major faults driving subsidence but also for exploring the links between tectonic processes and volcanic activity in the region. The tectonic structures in the plain may influence or even share dynamics with the volcanic activity observed at the margins of the plain. Exploration wells[11,12] drilled near the towns of Parete and Villa Literno (Fig. 1), a few km to the north of the Campi Flegrei Caldera, found massive volcanic deposits, matching with significant, intense magnetic and gravity anomalies in the southern plain, and suggest the presence of ancient volcanoes buried within the sediments of the plain[9].

A better understanding of the tectonic evolution of the Volturno Plain is also essential for clarifying its structural relationship with the adjacent volcanic complexes, including Campi Flegrei to the south and Roccamonfina to the north. Notably, Campi Flegrei, located about 15 km west of Naples, is one of the most active and hazardous volcanic regions in the world. Its history of frequent explosive eruptions and proximity to densely populated areas poses a significant risk, further emphasizing the importance of understanding the tectonic-volcanic interactions in this region.

Seismic data

Vectorization and analysis

The dataset used for this study consists of nineteen TIFF and PDF images of time-migrated seismic profiles, dating back more than forty years. The seismic lines were acquired between 1977 and 1988. Early profiles (fourteen, acquired in 1977, 1980 and 1981) used explosive charges (2–5 kg) placed in wells at depths of 16–26 m, with geophone arrays typically consisting of 48 to 60 groups spaced 50 m apart, each summing signals from 24 geophones. For the five profiles acquired in 1988, the number of geophone groups increased to 120 with 30-meter spacing, improving resolution and fold. These later recordings utilized four seismic vibrators with a 10-second, 12–70 Hz linear upsweep. Overall data quality is high, though it deteriorates below 2–3 s, Two-Way-Travel-Time (TWTT) due to limited CDP coverage, choice of swept frequencies, and use of 14-Hz vertical geophones combined with analog band-pass filtering (8–125 Hz, 18 dB/Oct.). Original processing involved initial steps such as data demultiplexing, amplitude correction to compensate for wavefront geometrical spreading and, when necessary, the definition of a crooked line geometry. Predictive deconvolution was a critical phase in this process, aiming at attenuating short-period multiples[38,39]. Deconvolution was followed by seismic velocity analysis, which is needed for the normal-moveout correction and common midpoint stack[38,39]. Subsequent refinement efforts focused on improving velocity models and CMP stacks through iterative cycles of residual statics corrections, complemented by further velocity analysis. Dip moveout correction, wavelet conversion from minimum to zero phase, and time-variant filtering completed the processing phase. A finite-differences time migration algorithm[40] was applied post-stack.

The initial phase of our work involved vectorizing the images using a code developed in MATLAB® by Sopher[41]. In contrast to other programs, Sopher[41] describes the method used for detecting trace baselines and identifying/removing timelines on the seismic image. Vectorization implies a certain degree of approximation (see Fig. 2); however, quantitative analysis of the method's performance shows that an average trace-to-trace correlation coefficient ranging from 0.8 to 0.95 can be attained for typical plotting styles[41]. The georeferenced vectorized profiles, in SEGY format, were subsequently imported into Landmark's SeisSpace processing suite for signal enhancement and conversion into depth using the original root mean square (RMS) velocity functions published in the TIFF images. Finally, the depth-converted, time-migrated seismic profiles were loaded into the open-source suite OpendTect® for interpretation. It is worth noting that depth conversion when solely based on surface P-wave velocity estimates, may be subject to an average error of 10%[38]. However, our interpretation of carbonate depths was calibrated with data from numerous exploration wells drilled in the plain, some of which are positioned along the seismic profiles.

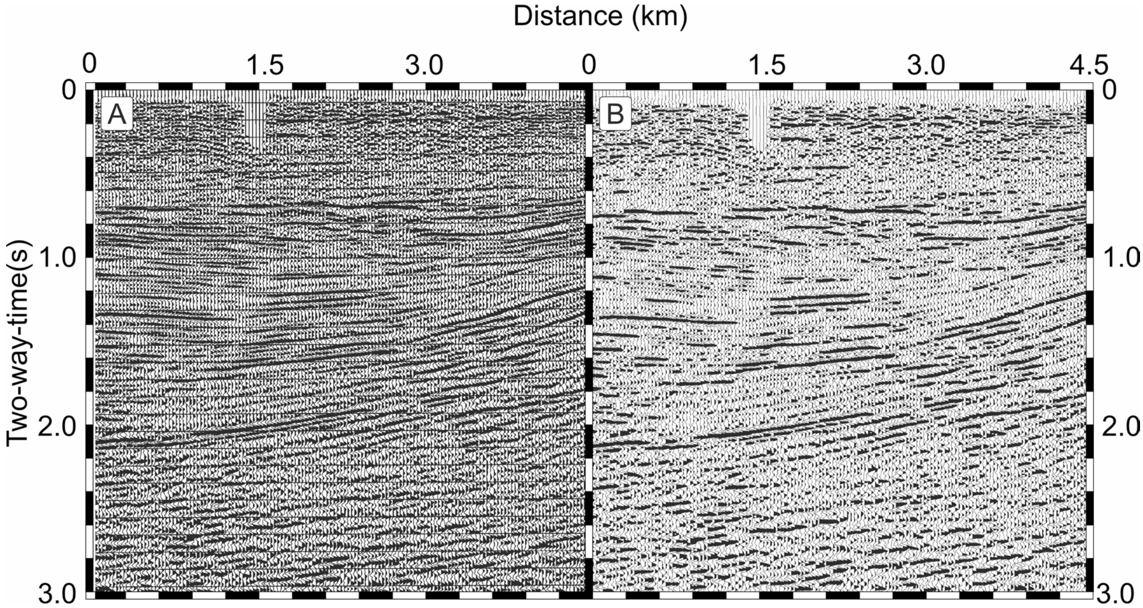

Fig. 2. Comparison between the seismic data in bitmap TIFF format (**A**) and the result of vectorization (**B**) achieved using a MATLAB code developed by Sopher[41]. Vectorized data are plotted in a style consistent with the input data. Notably, timelines present in the bitmap have been effectively removed during the process. While vectorization involves some level of approximation, the comparison reveals minimal differences between the two images.

Seismic data Interpretation

Our goals for this phase were identifying the top of the carbonate units of Upper Triassic to Early Miocene age and the main faults dissecting it. We have deliberately ignored the complication of the reflective sequence above the top of carbonates. Faults were interpreted only when seismic data showed consistent reflector offsets and amplitude reductions or anomalies along the fault surface. Identification criteria included abrupt changes in reflection patterns, truncations or displacements of reflections and, where present, growth strata in the hanging wall dipping toward the fault. Identifying the top carbonate on seismic data relies on analyzing its reflection characteristics and the configuration patterns of the reflectors above it. Seismically, this interface appears as a highly reflective event, marked by a few low-frequency cycles with variable energy[16]. Locally, this reflector shows unconformity relationships with the overlying, mainly continuous and parallel reflectors, which may represent: (a) sedimentary and pyroclastic sequences of Plio-Quaternary age, (b) Mio-Pliocene sediments, and (c) terrigenous successions, primarily of Tertiary age. This thick Quaternary-to-Tertiary sequence deposited above the carbonates has been penetrated by nearly all wells[9]. Stratigraphic data[11] show that this sequence exceeds 3300 m in thickness in the Volturno Plain. As the carbonate deepens, the signal-to-noise ratio decreases, making identification more challenging. Analyzing configuration patterns, cross-referencing with other seismic lines, and using data from numerous wells becomes crucial for distinguishing between various alternatives. Carbonate outcrops have served to constrain the depths of the basement.

To illustrate the tectonic style of the area, the reflectivity characteristics of the Meso-Cenozoic basement and the Plio-Quaternary fill of the Volturno Basin, we present interpretations of selected seismic profiles in Figs. 3, 4, 5 and 6. Our structural and stratigraphic interpretations of the post-stack time-migrated and depth-converted seismic images are based on comparisons of reflection character and configuration patterns. Our interpretation considers: (1) gravity and aeromagnetic data[42,43]; (2) P-wave seismic velocities derived from the analysis of the seismic profiles; and (3) litho-stratigraphic information from the numerous deep boreholes and related geophysical logs available in the area (Fig. 1: Ippolito et al.[11], Bernasconi et al.[12]). We also consider the geological, geophysical, and stratigraphic data collected in the Volturno Plain, published in both recent and older works[6,9,10,14,16,18,20,37,44–47]. Although[47] Plio-Pleistocene reflectors are not the primary focus of this study, the main unconformities have been highlighted in the interpreted seismic sections shown in Figs. 3, 4, 5 and 6.

Figure 3 shows Line 18, which intersects the only well that reaches the Meso-Cenozoic basement at a depth approximately 1.5 km below the surface. This profile clearly displays the basement's reflectivity characteristics, appearing as a relatively continuous doublet with a significantly lower frequency than the reflector package of the overlying basin fill. This reflector is generally associated with high P-wave velocities (V_{RMS} > 4000 m/s) and marks the top of a poorly reflective, low-frequency seismic zone below, characteristic of massive carbonate units. Aside from the probable boundary between Mesozoic and Miocene carbonates, we interpret that most of the reflectivity observed beneath the doublet is likely attributed to multiples that were not effectively attenuated during processing. As the basement deepens, particularly on the left side of the section, the signal-to-noise ratio decreases, making it more challenging to trace the basement's continuity. The profile also reveals a series of normal faults at approximately 2 km and 9–10 km along the line, dissecting the top of the carbonates. In some

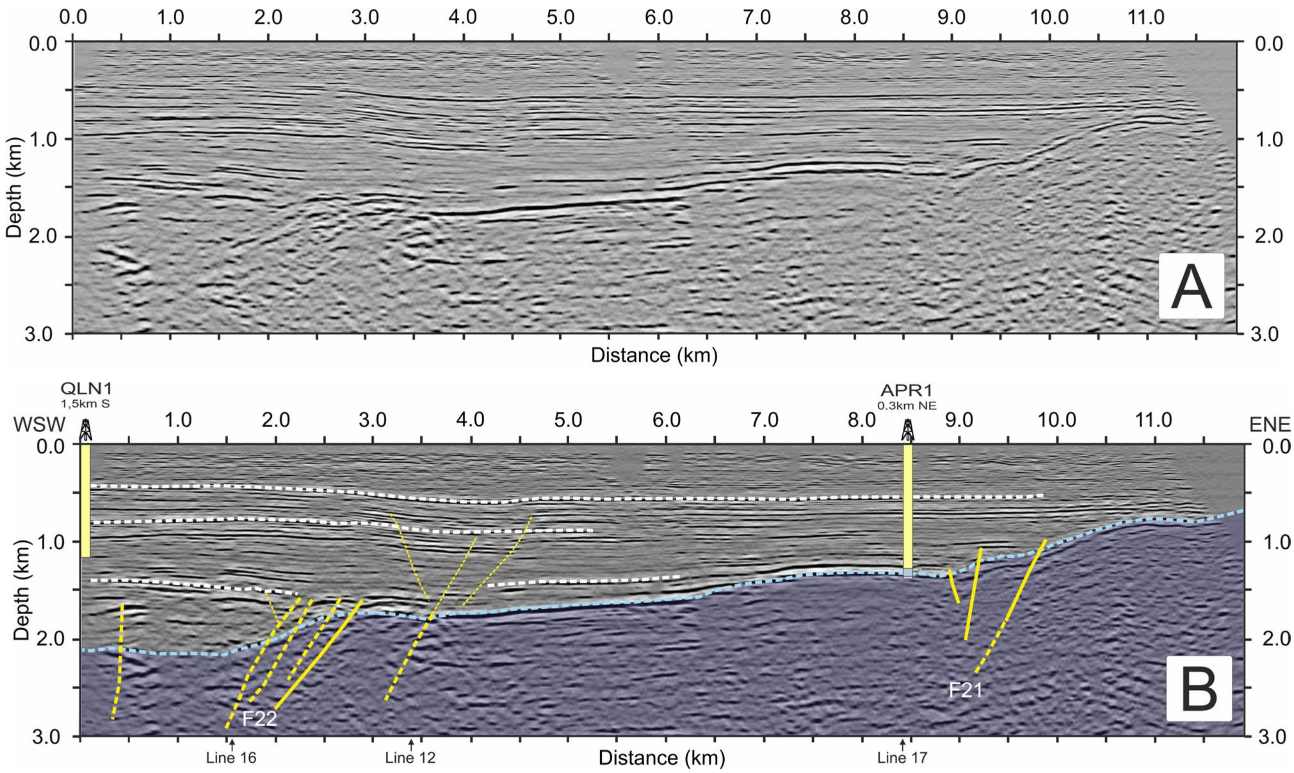

Fig. 3. **(A)** Grayscale image of the time-migrated and depth-converted Line 18. **(B)** Interpretation. In this and the following figures (4–6) yellow lines (dashed when uncertain) show interpreted faults; dashed white lines indicate major unconformities or the brightest reflectors in the upper Plio-Quaternary sequence; the Meso-Cenozoic carbonate basement is colored in blue. Well APR1 intersects this line at ~ 8.5 km. This is the only well in the Volturno area that penetrates the Meso-Cenozoic carbonate basement, reaching it ~ 1.5 km from the surface. The other well (QLN1), is projected onto the seismic profile, from 1.5 km to the south (see Fig. 1) and reaches a depth of 1.2 km within the Plio-Quaternary sequence (pale yellow).

cases, these faults extend into the overlying reflectors, though the decreasing offset prevents clear evidence of displacement.

Figure 4 shows a composite image combining parts of profiles 19 and 20, acquired along the coastline and intersecting the mouth of the Volturno River at a metric distance of 3.3 km. As evident from the geological map of Fig. 1, lines 19–20 run near Mt. Massico horst, located to the north of the map. The composite seismic section reveals a network of low-angle, anastomosing normal faults with a listric geometry, downthrowing the Meso-Cenozoic basement from a few hundred meters at the start of the line to over 5 km at approximately 12 km. The overlying sediments are deformed due to fault activity, particularly showing a well-defined reverse drag between 2 and 5 km along the profile. Additionally, this image confirms that when the carbonate basement is deeply buried, poor signal-to-noise ratios complicate the ability to trace its continuity on the seismic profiles, making interpretation more challenging, as also discussed above, implying that constraints (wells and tie-lines) are fundamental for the interpretation.

Figure 5 presents the interpretation of Line 10, which trends NNW (see Fig. 1). The profile reveals a fault zone (F2-F4) south of Mt. Massico, corresponding to the same fault shown in Fig. 4, hereafter referred to as the Mt. Massico Fault. This fault zone rapidly downthrows the carbonate basement towards the SE, reaching depths exceeding 5 km. The basement then gradually rises to the south, defining a half-graben, with the master fault being Mt. Massico Fault. Despite the similarity in azimuth between this profile and the composite profile in Fig. 4 and a lateral spacing of about 3 km, the low-angle fault visible in the previous profile appears steeper here. This discrepancy suggests either a change in the strike of the Mt. Massico Fault near the coast, leading to an inaccurate representation of its true dip, or a significant decrease in fault dip near the coastline.

The previous interpretation is supported by the interpretation of Line 7 (Fig. 6), which starts approximately 5 km south of Mt. Massico massif and runs NW-SE, terminating SW near the town of Grazzanise (see Fig. 1). Line 7 intersects Line 10 at approximately 4.5 km and the tectonic framework revealed is very similar to that of the previous profile, confirming the presence of a fault zone south of Mt. Massico, as clearly depicted in Fig. 4. Here our interpretation shows the half-graben structure from a slightly different azimuth, with the basement gradually rising towards the SE and reaching a minimum depth of 1.6 km below well QLN1, about 1.5 km to the south of the town of Villa Literno. Like the previous profile, this line intersects or is close to several exploration wells, which are crucial in defining a minimum depth for the carbonate basement, thereby reinforcing the reliability of the seismic interpretation regarding basement depth. As with the previous profile, but more

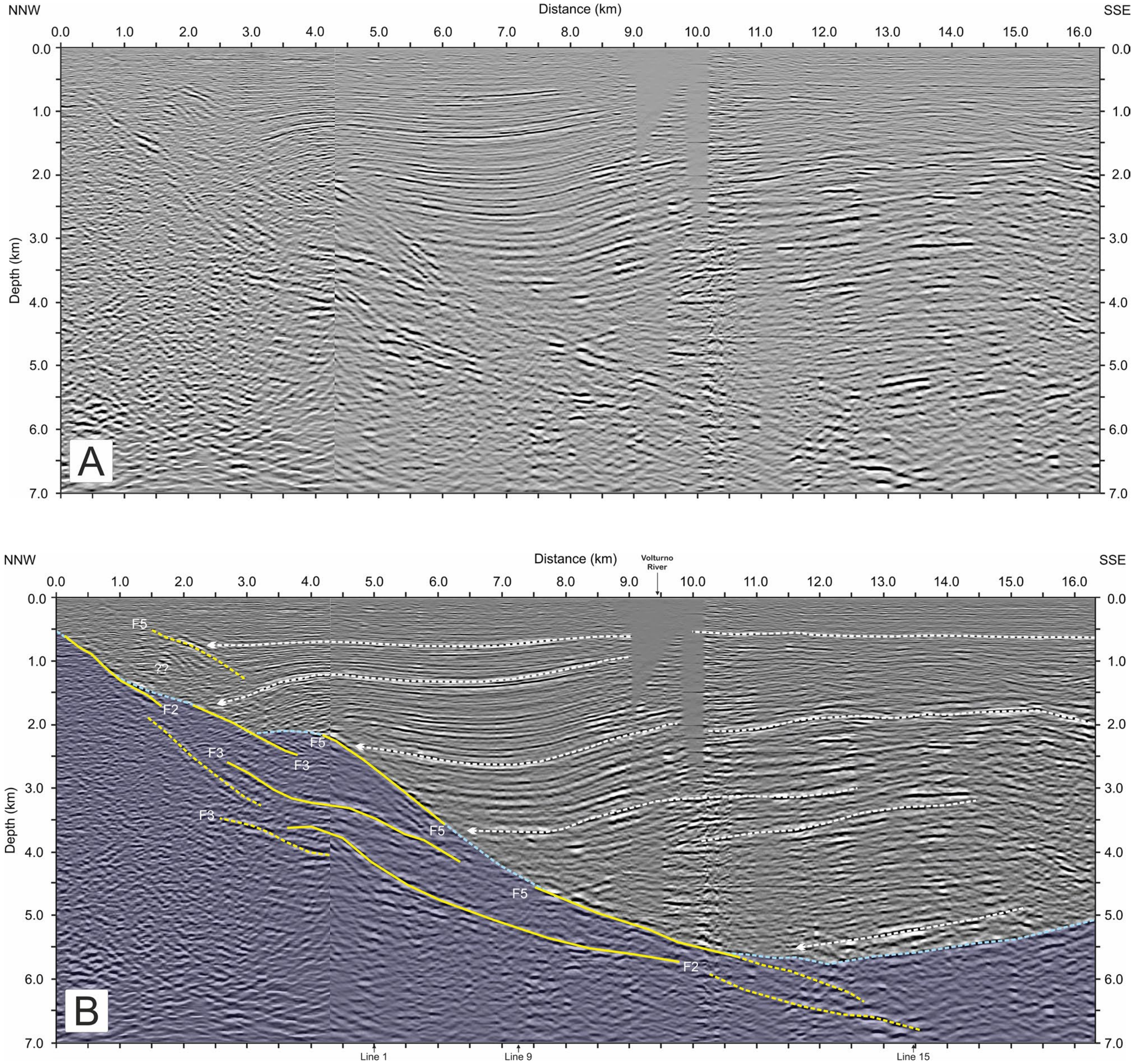

Fig. 4. (**A**) Grayscale seismic image combining parts of Lines 19 and 20 across the Volturno River mouth (with overlapping areas removed). **(B)** Interpretation of seismic data. The seismic image reveals a set of low-angle anastomosing normal faults that form a broad fault zone, causing the Meso-Cenozoic carbonate basement (blue) to subside by more than 5 km south of the Mt. Massico outcrops. Symbols: F2, F3, F5, major faults;'??', features of uncertain interpretation. For other symbols see the caption of Fig. 1.

distinctly in this line, the Plio-Pleistocene basin fill overlying the carbonate basement is significantly deformed and includes several unconformities and bright spots, the latter likely originating from volcanic deposits, as suggested by well stratigraphy of QLN1.

Figure 7A shows, as an image map, overlaid by contour lines, the gridded depths of the Meso-Cenozoic basement in the Volturno Plain, derived from seismic profiles (white dashed lines) and constrained by basement outcrops (black dots) at NW (Mt. Massico), N and E (Caserta Mountains). Basement depths interpreted from the seismic profiles and outcrop data were interpolated using a kriging algorithm[48]. Approximately 12,000 points were interpolated into a grid of 9,292 nodes, with spacing of 101 m (easting) and 92 m (northing), covering 872 km² and including the Volturno Plain and parts of the Massico and Caserta Mountains (Fig. 1).

This map reveals that the carbonate basement is primarily controlled by NE- and NW-trending fault systems. The main fault system responsible for most of the subsidence in the plain is composed of the Mt. Massico Fault System, made of a set of anastomosing normal faults (F1-F5), well evident on profiles 19 and 20 (Fig. 4) and forming a broad fault zone predominantly NE-striking, located SW of the Massico horst. This fault system causes the Meso-Cenozoic carbonate basement to subside by more than 5 km at about 10 km south of Mt. Massico. It should be considered the master fault system of the Volturno half-graben.

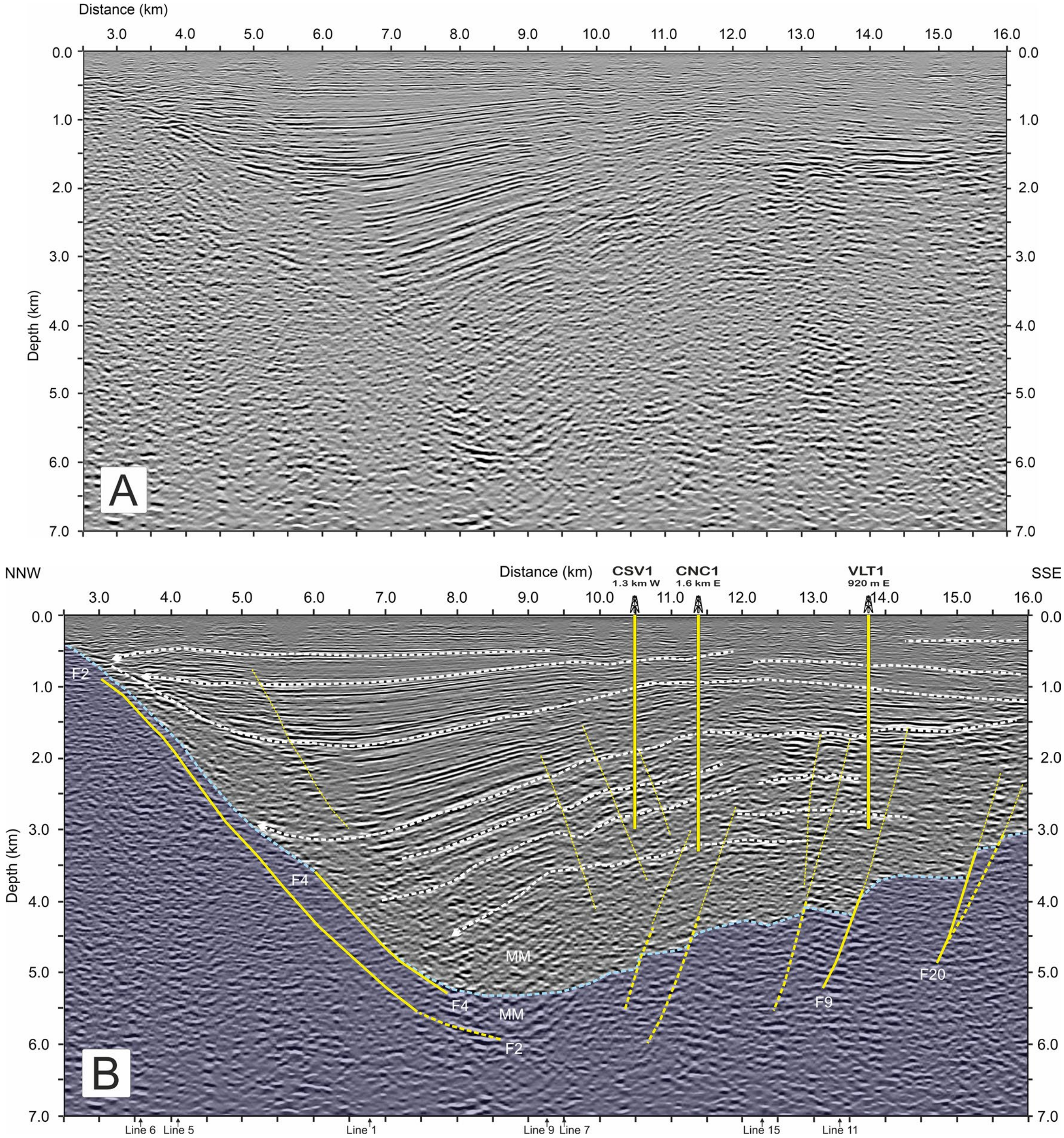

Fig. 5. (**A**) Grayscale image of a particular of the time-migrated and depth-converted Line 10. **(B)** Interpretation. This line is situated near two clusters of exploration wells, which reach a maximum depth of ~ 3300 m (CNC1), though none penetrates the Meso-Cenozoic carbonate basement. Symbols: MM; multiples; F2, F4, F9, F20; major faults. For other symbols see the caption of Fig. 1.

Figure 7A also shows that the deepest part of the Volturno graben (> 5000 m) lies about 3 km north of the current Volturno River mouth. Faults F1-F5 accommodate most of the vertical displacement of the half-graben as evident in the seismic profiles (Figs. 3, 4, 5, 6 and 7), while NE-trending, NW-verging faults (F9, F10, F18-to-F24), bounding to the SE the area of maximum subsidence (> 3000 m, in blue tones in Fig. 7A) are here interpreted as secondary, conjugate structures to the main SE-verging fault system (F1-F5). Additionally, NW-trending faults (F7–F15) appear less frequent and are considered a subordinate system contributing to the subsidence of the carbonate basement from the Caserta Mountains toward the depocenter.

Potential Field data Analysis and Interpretation

Gravity data

The Bouguer anomalies in the Volturno Plain area were digitized from the Gravity anomaly map of Italy[42] and gridded at a regular step of 500 m. The gravity data were separated into regional and local (residual) components using a first order regression. The regional component approximates the gravity component of deep origin, presumably related to the deepening of the Moho from the Tyrrhenian area (SW) to the Apennine chain axis (NE), creating an evident SW-NE decrease of the gravity values in this area. After subtraction of the regional

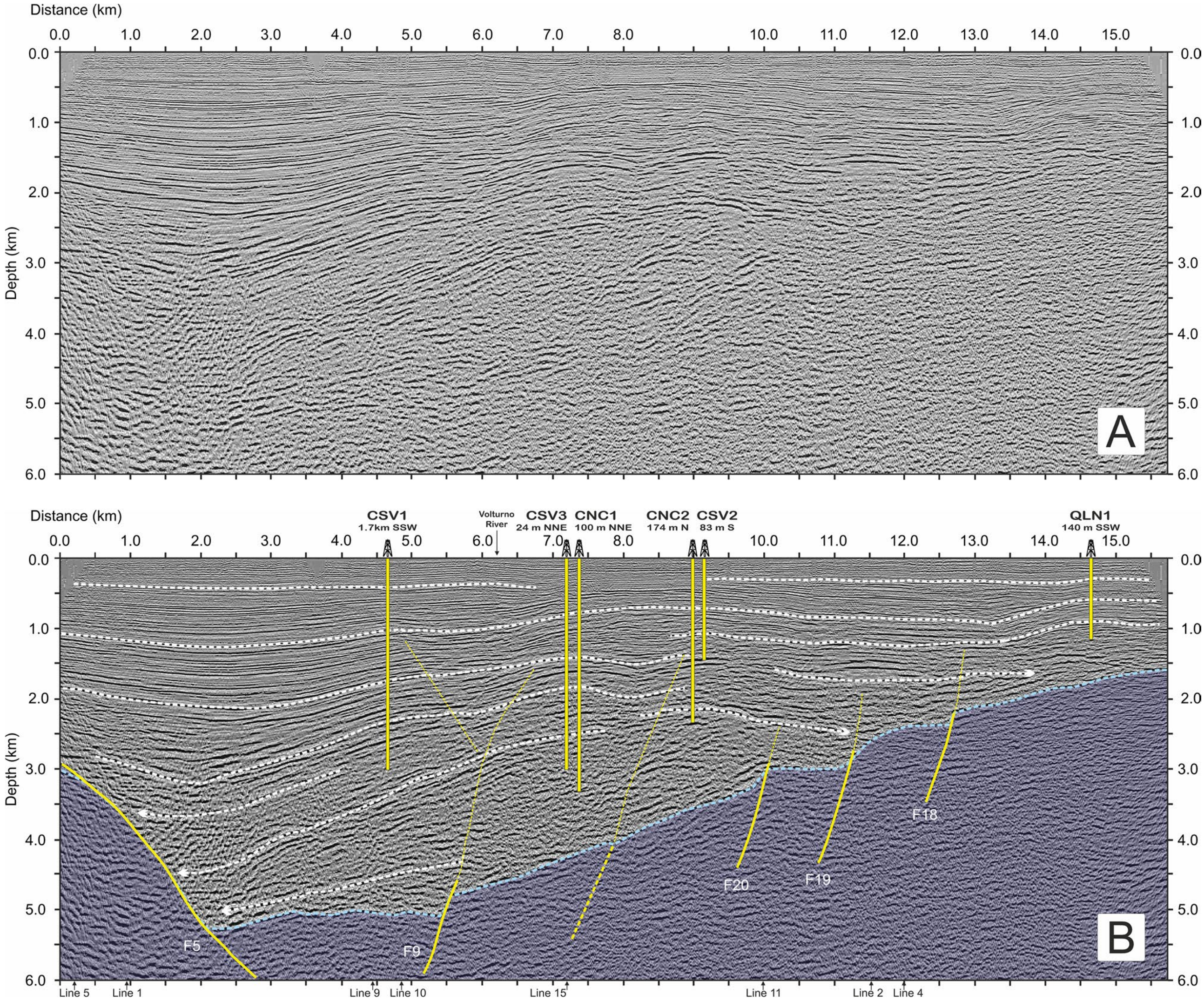

Fig. 6. **(A)** Grayscale image of the time-migrated and depth-converted Line 7. **(B)** Interpretation. Like the previous profile, this line also intersects or is near several exploration wells, with a maximum depth of ~ 3300 m (CNC1), though none of the wells reach the Meso-Cenozoic carbonate basement. Symbols: F5, F9, F18-F20; major faults. For other symbols see the caption of Fig. 1.

component from the original data, the residual field shows local components that appear more tightly related to shallow sources (Fig. 7B). The main feature is a gravity low of amplitude about 20 mGal located on the west side of the study area (A in Fig. 7B), corresponding to the lower course of the Volturno River, about 7 km upstream from its estuary in the Tyrrhenian Sea. This gravity low extends slightly eastward, forming a pronounced branch (A'). It is bounded by gravity highs associated with the foothills of the Apennine Chain, specifically Mt. Massico to the north and the Trebulani/Tifatini Mountains to the east. This gravity low is interpreted as resulting from the subsidence of the carbonate basement, which outcrops to the north and east, and is marked by strong gravity highs. The low is caused by the density contrast between the carbonate series and the marine, fluvial, and volcanoclastic sediments filling the basin. In the southern Volturno Plain, the gravity field shows local highs (B and C in Fig. 7B) likely related to buried massive igneous bodies identified in exploratory wells PRT2 and VLL1[9,11,50]. Other gravity highs in this region (e.g., D in Fig. 7B) can be instead attributed to buried carbonate horsts, as suggested by magnetic data analysis (Fig. 8A). In the northern part of the study area, east of Mt. Massico, the residual gravity map reveals a southwest-elongated high (E in Fig. 7B), corresponding to the buried portion of a carbonate ridge. Northwest of this ridge, a gravity low (F) extends northwards, connecting the Volturno Basin with another tectonic depression that hosts the Roccamonfina volcanic complex[51].

We applied enhancement methods to the residual gravity field shown in Fig. 7B to delineate the edges of the gravity sources. Specifically, we employed a high-resolution boundary estimator based on the horizontal derivative technique, known as the Enhanced Horizontal Derivative (EHD; Fedi and Florio[52]). The EHD is defined as the amplitude of the horizontal derivative of a summation of vertical derivatives of various orders of the gravity field, each weighted according to schemes designed to selectively enhance different features of the original field. Like other boundary detection methods, EHD highlights the lateral edges of gravity sources

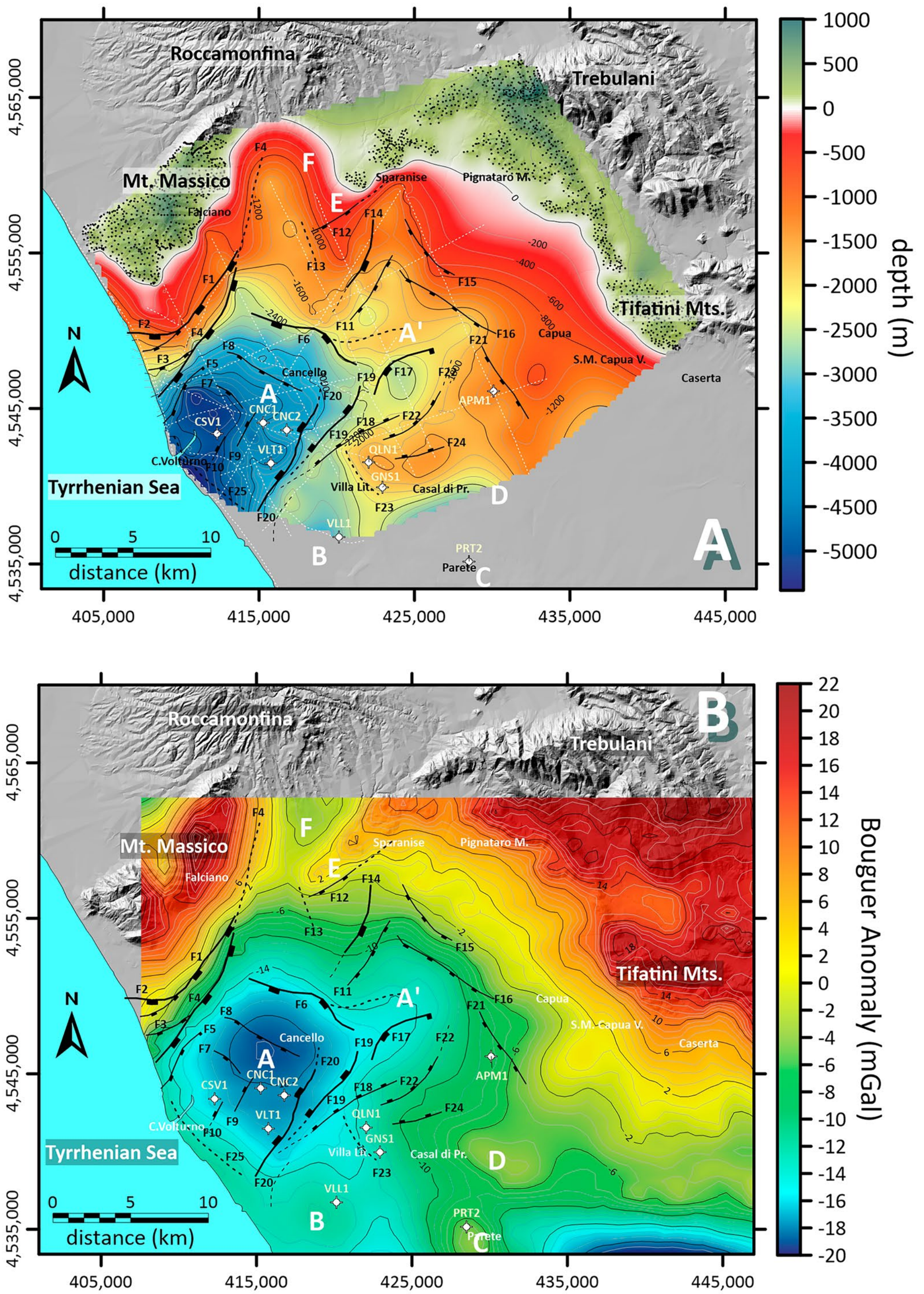

Fig. 7. **(A)** Contour map of Meso-Cenozoic basement depths in the Volturno Plain, derived from interpolated seismic profile data (white dashed lines) and constrained by basement outcrops (black dots) at Mt. Massico (NW) and the Caserta Mountains (NE, E). **(B)** Contour map of the residual Bouguer anomaly, digitized from the Gravity Anomaly Map of Italy (Carrozzo et al.[42]) and gridded at 500 m intervals. Both maps include shaded relief from DEM data[49], exploration wells (white dots), and fault strikes interpreted from seismic data (ticks mark the downthrown side). The coordinate system is WGS84 UTM Zone 33 N. This map was generated with Surfer (www.goldensoftware.com), version n. 27 (2024).

through its maxima, enabling fast and preliminary mapping of concealed geological features. However, unlike other techniques, EHD may implement a Multiscale Derivative Analysis (MDA; Fedi[53]), acting as a filtering process without explicitly separating field components. By carefully selecting and weighting derivatives of different orders, EHD can enhance the gravity field at specific scales (e.g., local, intermediate, or regional). For the

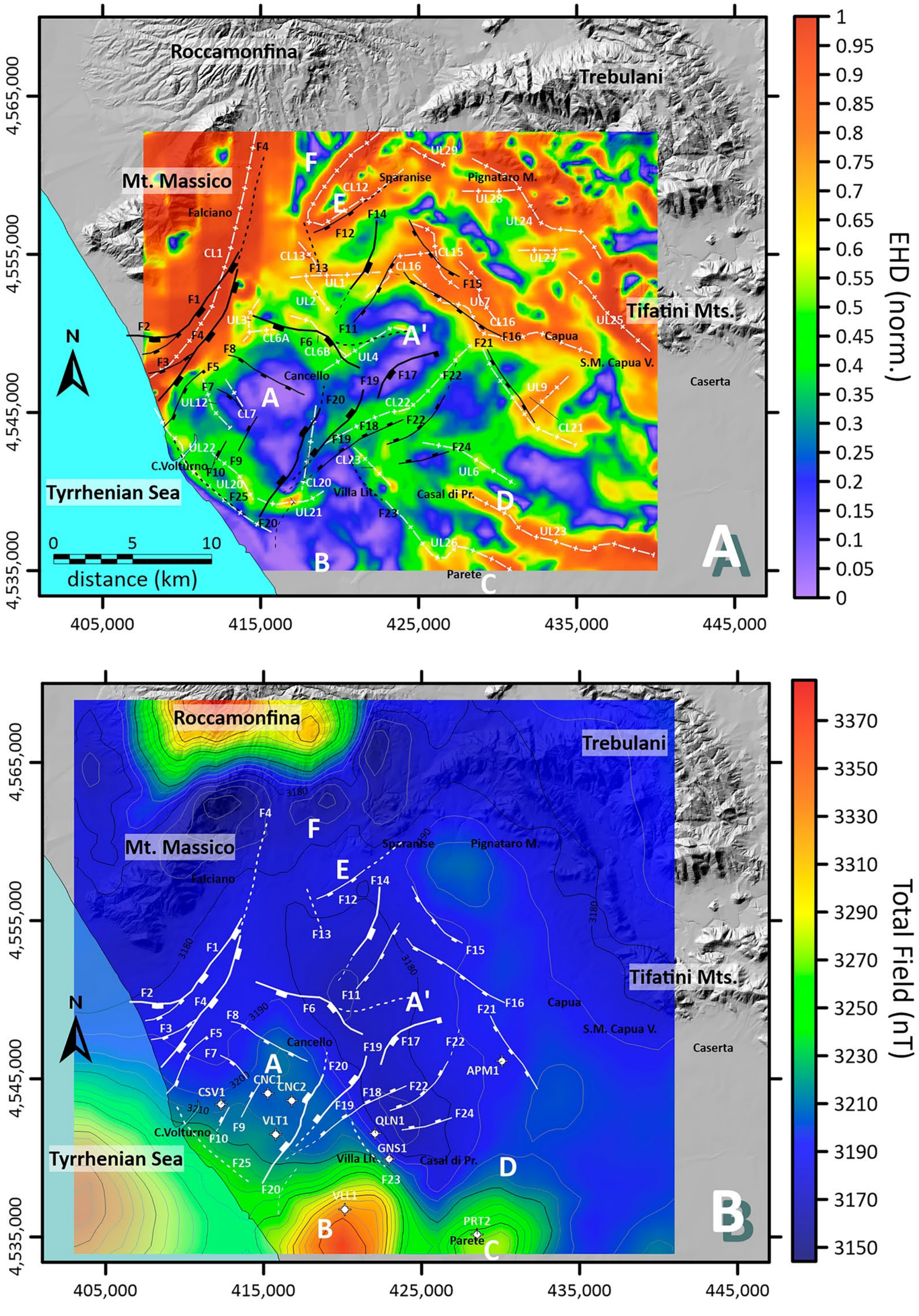

Fig. 8. **(A)** Image map of the Enhanced Horizontal Derivative (EHD; Fedi and Florio[52]), with values normalized between 0 and 1. EHD maxima are indicated by long dashes and plus signs. Maxima labeled "CL" correlate with faults from seismic and other data, while "UL" remain uncorrelated. **(B)** Contour map of aeromagnetic data for the Volturno Plain, digitized from AGIP maps (1:500,000 scale[43]), and gridded at 2000 m intervals. Both maps include shaded relief from DEM data[49], exploration wells (white dots), and fault strikes from seismic interpretation (ticks mark the downthrown side). This map was generated with Surfer (www.goldensoftware.com), version n. 27 (2024).

residual gravity field in Fig. 7B, we focused on enhancing intermediate-scale features by incorporating second- to fourth-order derivatives with unit weights in the EHD computation. The EHD map is shown in Fig. 8B. The EHD edges often coincide with tectonic structures, particularly where geological formations with contrasting densities are in lateral contact (e.g., the Meso-Cenozoic carbonate basement and marine or continental deposits).

Magnetic data

The aeromagnetic dataset for the Volturno Plain was digitized from AGIP maps at a 1:500,000 scale[43] relative to an altitude of 2590 m above sea level and subsequently interpolated onto a regular grid with a 2000 m spacing. The dataset was reduced to the pole, so minimizing the offset between anomaly features and source positions, using the local average IGRF direction for both the inducing field and total magnetization vectors (Fig. 8B).

The reduced-to-the-pole total field in Fig. 8B is relatively flat in all of the Volturno plain, with the significant exceptions of strong magnetic anomalies along its northern and southern boundaries. Northern anomalies (north of F in Fig. 8B) are clearly associated with the presence of igneous products originating from the Roccamonfina volcanic complex. In contrast, the southern anomalies B and C (coincident with gravity anomalies) can be interpreted as related to the easternmost part of the "41 st parallel" magnetic lineament, a > 200 km long transform zone separating the northern and the southern Thyrrenian basins[16,31,54]. Exploratory wells (QLN1, PRT2, VLL1, and GNS; Fig. 8B) drilled near or in correspondence to the southern anomalies confirm the presence of igneous bodies, including lava and pyroclastic deposits, embedded within the sediments of the Volturno Plain. Notably, the stratigraphy of wells PRT2 and VLL1, located close to the centers of anomalies B and C in Fig. 8B, reveal more than 1600 m thick andesitic lavas[50]. As can be noticed in Fig. 8B, the magnetic anomaly in the Villa Literno area (B) is more intense than that in the Parete area (C). As said above, the presence of these dense lava bodies also generates gravity highs; however, in this case the strongest gravity anomaly is that in the Parete area (anomaly C in Fig. 7B). On the other hand, gravity high D, located about 5 km north of magnetic anomaly C, does not coincide with any magnetic anomaly, suggesting that its source has a non-igneous nature and it is likely generated by a carbonate basement high.

Comparative analysis of results

The comparison between the gravity anomalies and the depth map to the carbonate basement (Fig. 7) reveals significant similarities. First, the gravity low observed north the mouth of the Volturno River has a similar shape to that of the carbonate basement low derived by the interpretation of seismic data. Notably, the gravity minimum does not align perfectly with the maximum depth of the carbonate basement estimated from seismic data, instead being offset by approximately 3 km to the northeast. This discrepancy may result from heterogeneities in the sediments filling the plain (e.g., cemented breccias, carbonate olistostromes), which cause variations in relative density and consequently affect the gravity response. One significant feature identified through seismic and gravity data is a north-elongated low in both maps ("F" in Fig. 7), which links the Volturno Plain to the Roccamonfina volcano. This feature, which could be interpreted as a graben, is flanked by Mt. Massico to the west and by the NE-trending carbonate ridge of the Trebulani Mountains ("E" in Fig. 7) to the east. Some differences in shape between the two maps, including the less pronounced secondary minimum A' in the seismic data, can be attributed to the different areal data distribution of gravity and seismic data. The carbonate basement depth map was created by interpolating depth data sampled along seismic profiles irregularly distributed in the Volturno plain. In fact, the regions not crossed by seismic lines are sometimes significant in extent. In contrast, the gravity anomaly was more homogeneously sampled, providing a more uniform coverage of the Volturno Plain area.

To facilitate comparison, the fault pattern interpreted from seismic data was overlaid onto the gravity and magnetic maps. This reveals that the interpreted NE- and NW-trending tectonic structures bound nearly all gravity features, including the A–A' minimum. Moreover, the A–A' gravity low exhibits contour lines aligned in NE and NW directions. The same pattern is observed in the gravity high bounding Mt. Massico to the northwest. Additionally, the plain area adjacent to the Caserta Mountains shows a clear NE trend in the Bouguer Anomaly, closely following the NE trend of the carbonate basement. This alignment provides further evidence supporting the existence of NE- and NW-oriented tectonic structures in the Volturno Plain.

To assess the consistency of fault strikes interpreted from seismic profiles with gravity data, we compared them to the lateral edges of gravity sources identified by EHD maxima in Fig. 8A. It can be observed that most maximum amplitude trends of the EHD ("CL" in Fig. 8A) align well with the major fault lines inferred from seismic data. However, some linear trends of EHD maxima run parallel to certain faults but are consistently offset by a fixed distance relative to them. (e.g., F18-19–22 and CL22 in Fig. 8A). This horizontal shift between an EHD maxima trend and a mapped fault has been observed in similar structural settings[37,55]. This phenomenon is particularly evident for trends CL1 (partially), CL18, CL21, and CL22 in Fig. 8A and can be explained by the fact that for non-vertical faults, the EHD maxima trends are offset from the fault's outcropping trace towards the dipping direction. Thus, these trends do not correspond to the fault position at the surface but exhibit an offset that increases with the fault throw and decreases with the dip angle[56]. Additionally, it should be noted that several linear trends of EHD maxima (labeled "UL" in Fig. 8A) are visible in areas where no faults are mapped based on seismic interpretation. This may occur either because some tectonic features remain undetected (e.g., areas not sampled by seismic profiles) or because the EHD highlights lateral density contrasts unrelated to faults. Nonetheless, the EHD map has proven to be a valuable tool for supporting structural interpretation of seismic profiles, as it confirms the presence of structural elements while also enabling the mapping of lateral extents of features that are hidden or visible only in limited areas along seismic profiles.

A further comparison of gravity and seismic data with the reduced-to-the-pole magnetic map shown in Fig. 8B reveals several shared features across the three datasets. Aside from the magnetic anomalies attributed to the Roccamonfina volcanic complex in the north and the strongly magnetized lava bodies in the Villa Literno and Parete areas in the south, the Volturno Plain, including the area characterized by maximum basement subsidence, shows magnetic field anomalies of very low amplitude. This map thus enables the clear delineation of the basin fill, consisting predominantly of low-magnetization lacustrine and alluvial sediments, and areas containing highly magnetized lava bodies. As for gravity data, also magnetic anomalies in the map display boundaries mainly oriented in NE and NW directions. Notably, the magnetic highs B and C to the south, linked to the easternmost extent of the 41st parallel magnetic feature, likely indicate that volcanic activity related to the opening of the Tyrrhenian basin also occurred onshore, just north of the Campi Flegrei volcanic district and is presently buried under several hundred meters of Quaternary sediments.

Discussion and Conclusions

This study describes a multidisciplinary approach employed to investigate the tectonic and subsurface settings of the Volturno Plain by integrating vintage seismic reflection profiles, gravity and magnetic data. It demonstrates the value of legacy data combined with modern multidisciplinary analysis and interpretation techniques in unraveling the subsurface of large alluvial plains. Our findings provide a reliable tectonic framework for the Volturno Plain and highlight potential links to volcanism. The combined analysis of seismic profiles and gravity data allowed us to define a system of predominantly NE- and NW-trending normal faults that control the deep subsidence of the Meso-Cenozoic carbonate basement. These findings are summarized in the tectonic maps presented in Fig. 9. The faults depicted in this figure slightly differ from those in earlier figures, as they integrate the comparative analysis of seismic data and EHD trends obtained from gravity data (see Figs. 7 and 8). The EHD analysis was particularly useful for verifying the strike of many faults interpreted from 2D seismic profiles data and, in several cases, extending tectonic structures into areas not covered by seismic lines.

Our revised fault architecture accommodates basement displacements exceeding 5 km beneath the Volturno river delta, defining a half-graben system. These faults, consistent with NW- and NE-striking regional subsidence trends observed along the Tyrrhenian margin[6–8,18], drive the downward displacement of the Meso-Cenozoic carbonate rocks towards the coast. Our findings align with morphotectonic and mesostructural analysis of Mt. Massico and Caserta Mountains[3,20,35]. Fault displacement at Mt. Massico (slip rates: 2–2.5 mm/yr from 1.45 Ma to 0.36 ka and 0.2–0.5 mm/yr from 36 ka to present; Cinque et al.[57]) reaches several hundred meters, juxtaposing Quaternary deposits of the plain against carbonate and siliciclastic units. Notably, Mt. Massico's Late Quaternary evolution reflects the Tyrrhenian margin's E-W extensional regime[3,8]. Stratigraphic[58] and remote sensing data[34,59], confirm ongoing extensional kinematics in the plain.

To further contextualize our fault interpretation, we compared it with the fault network mapped by Vitale and Ciarcia[20], shown in white in Fig. 9A. Their map integrates decades of studies (see references in Vitale and Ciarcia[20]), reinterpretations of 1:100,000 and 1:50,000 geological maps[15,60], and original field surveys. Completely covered by Quaternary sediments and lacking significant bedrock outcrops, the Volturno Plain's mapped faults are necessarily inferred from geophysical and remote-sensing analyses rather than direct outcrop observations. While most E-W faults they report in the Volturno Plain are inconsistent with the NE and NW fault trends revealed by our data, their NE- and NW-trending faults generally align with or extend the trends of our faults. Notably, their NE- and N-trending faults south of Mt. Massico correspond to our Mt. Massico Fault System, particularly splays F1 and F4, while their NE-trending fault near Villa Literno partly aligns with our Villa Literno Fault System (i.e., F19, F18, E18, F22).

Figure 9A presents a color map of cumulative vertical ground displacement (1992–2010; see Buffardi et al.[61]), derived from InSAR measurements[34]. Displacement patterns roughly align with our major NE and NW fault trends, though smaller-scale eastward and northward trends are superimposed. Subsidence maxima do not perfectly overlap to the main plain depocenters inferred by seismic interpretation or to gravity lows (labels A–F: Fig. 9A). The Volturno Plain currently exhibits subsidence rates up to 16 mm/year, far exceeding long-term tectonic slip rates (~ 0.5-to-1 mm/year[35,57]). While tectonic subsidence contributes to cumulative vertical displacement, present-day deformation appears largely driven by non-tectonic processes such as sediment compaction, groundwater extraction, and other anthropogenic activities[34], as often observed in sedimentary basins subjected to human-induced stresses. Our findings suggest that non-tectonic processes primarily drive short-wavelength deformations, while tectonic processes control broader-scale patterns. Therefore, tectonic subsidence remains active, primarily controlled by two NE-trending fault zones, the Mt. Massico Fault System (i.e., F1-to-F5) and the Villa Literno Fault System (i.e., F19, F18, E18, F22) (Fig. 9B). This interpretation is consistent with the results of Luiso et al.[37], who documented ongoing fault activity at Mt. Massico since the Plio-Pleistocene, characterized by low-energy earthquakes ($Mw \leq 4.8$). The Mt. Massico and Villa Literno faults likely contribute to present-day deformation through aseismic creep and low-magnitude seismicity.

Figure 9B compares the main tectonic structures identified in this study with epicentres of instrumental (1985–2024, ISIDe Working Group[62]) and historical earthquakes (ASMI-CPTI: Rovida et al.[63]). The sparse and low-magnitude seismicity observed supports the hypothesis that present-day deformation along these fault systems is mainly aseismic. Insets display polar histograms of fault orientations, comparing our results (histogram a) with the faults reported by Vitale and Ciarcia[20] (histogram b), most of which were identified at the outcrop scale, particularly in Mt. Massico, the Tifatini Mountains, and the Trebulani Mountains. Some of these faults are depicted in white in Fig. 9A. Both histograms account for fault length, though the inferred Volturno Plain faults from Vitale and Ciarcia[20] are not included. Our dataset reveals consistent dominant trends aligned with NW and NE directions, in agreement with the regional tectonic framework. While Vitale and Ciarcia's[20] field data, offering high-resolution measurements at the outcrop scale, predominantly show NW trends, our broader spatial coverage allows for the identification of additional structural trends, particularly a pronounced NE orientation not as strongly represented in field observations. This difference likely stems from the ability of geophysical methods to detect buried NE-trending structures that may be poorly exposed at the surface. Although field data provide essential ground-truth validation, the integration of seismic, gravity, and magnetic

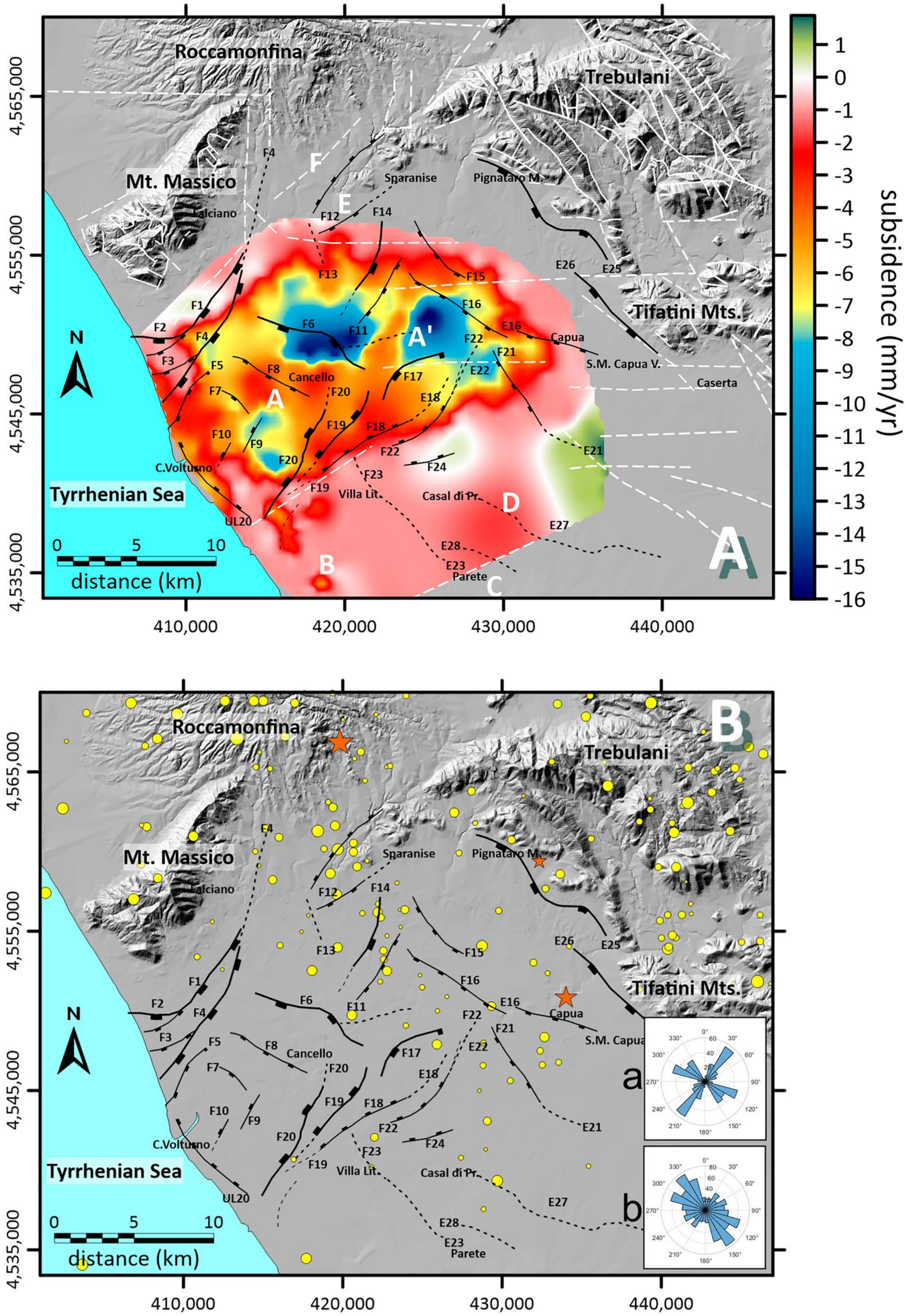

Fig. 9. **(A)** Image map of cumulative vertical ground displacement (1992–2010) from InSAR measurements[61], based on Persistent Scatterer interferometry datasets (Matano et al.[34]). Fault segments mapped by Vitale and Ciarcia[20] are in white; inferred faults are dashed. **(B)** Updated tectonic map of the Volturno Plain. In areas lacking seismic coverage, faults identified solely from EHD maxima are labeled with an "E" prefix (e.g., E25–E28). Insets show rose diagrams of fault orientations. Yellow circles and orange stars represent instrumental (1985–2024, ISIDe Working Group[62]) and historical earthquake epicenters (ASMI-CPTI catalog: Rovida et al.[63]), including the 1960 Mw 5.2 Roccamonfina, 1457 Mw 4.4 Capua, and 1950 Mw 3.7 Pignataro Maggiore events. Symbol size is proportional to magnitude. Both maps include shaded relief from DEM data[49] and fault strikes interpreted in this study (black, with ticks marking the downthrown side). This map was generated with Surfer (www.goldensoftware.com), version n. 27 (2024).

analyses in this study highlights the dominant role of NE-trending faults in shaping the geometry and evolution of the Volturno half-graben, providing a complementary regional perspective on fault distribution.

The significance of the NE-trending faults extends beyond the Volturno Plain, as they appear to influence broader regional tectonic and magmatic processes in the whole Tyrrhenian margin. Their role in controlling Campanian volcanism is well established[8,16,64–70]. Acocella and Funiciello[71], suggest that NE transtensive structures act as transfer faults accommodating differential extension within the stretched Tyrrhenian crust. According to them, these structures influence magma emplacement by: (1) forming extensional basins where decompression promotes magma accumulation at NW and NE fault intersections, leading to central volcanoes; and (2) enhancing permeability through strike-slip motion, facilitating fissure eruptions. While regional NW extension drives magma ascent, NE-trending faults play a critical role in controlling its emplacement at shallower levels.

Similar tectonic-magmatic interactions such as those in the Volturno Plain are observed further north. Roccamonfina volcano sits at the intersection of a NW-trending depression and the NE-oriented Garigliano graben, whose Early Pleistocene evolution was controlled by the Northern Mt. Massico Fault[51]. Colli Albani volcanism takes place at the intersection of NW faults within a N-S shear zone[72]. In Larderello, NE-trending transfer zones accommodate deformation, forming pull-apart basins that localize magmatism[73]. Mt. Amiata's Pleistocene volcanic centers align NE, consistent with trends controlling other Italian volcanic fields[74]. These examples are in line with Acocella and Funiciello's[71] view that NE-trending transfer zones are key to volcanic evolution along the Tyrrhenian margin.

Additional evidence comes from NE- and NW-oriented gravity and magnetic highs identified in the southern Volturno Plain, near Campi Flegrei. In this sector, exploration wells PRT2 and VLL1[30,50] reveal ~2000 m of Pliocene-Quaternary volcanic deposits. These are interbedded with alluvial and marine sediments in the wells to the north of the town of Villa Literno (e.g., QLN1), reflecting the interplay between magmatic activity and tectonic subsidence, particularly high during the Quaternary[10]. Thick volcanic sequences correlate with gravity and magnetic anomalies and suggest buried volcanic edifices, as proposed by Ortolani and Aprile[9]. This volcanic activity, localized in the southern part of the plain where NE- and NW-trending regional faults intersect the 41st Parallel Lineament, is consistent with large-scale features observed at Campi Flegrei, where the caldera is also structured along NE- and NW-trending fault systems, with NE-trending transfer structures playing a primary role[64].

Our findings confirm that the Phlegraean volcanic system, both continental and insular, developed along a NE-trending structural high[30], bounded by two half-grabens: the Volturno Plain (controlled by the NE-trending Mt. Massico Fault System) and the Gulf of Naples (controlled by the NE-trending Magnaghi-Sebeto Fault[31,66,70,75].

Data availability
Gravity and Magnetic data sets generated during the current study are available from the corresponding author on reasonable request. Restrictions apply to the seismic reflection data used for the current study, which are not publicly available.

Received: 8 January 2025; Accepted: 22 May 2025
Published online: 01 July 2025

References
1. Cortini, M., Roberti, N. & Scandone, R. Geocronologia e paleomagnetismo Del Vulcano Di Roccamonfina. *Ann. Geof.* **28**, 129–138 (1976).
2. Rouchon, V., Gillot, P. Y., Quidelleur, X., Chiesa, S. & Floris, B. Temporal evolution of the Roccamonfina volcanic complex (Pleistocene), central Italy. *J. Volcanol. Geoth. Res.* **177** (2), 500–514 (2008).
3. Billi, A., Bosi, V. & De Meo, A. Caratterizzazione strutturale Del Rilievo Del M. Massico Nell'ambito Dell'evoluzione quaternaria Delle depressioni costiere dei Fiumi Garigliano e Volturno (Campania Settentrionale). *Il Quaternario*. **10** (1), 15–26 (1997).
4. Putignano, M. L., Ruberti, D., Tescione, M. & Vigliotti, M. Evoluzione Tardo quaternaria Del margine Casertano Della Piana Campana (Italia meridionale). *Boll Soc. Geol. It.* **126** (1), 11–24 (2007).
5. Orsi, G., D'Antonio, M. & Civetta, L. (eds) *Campi Flegrei: A Restless Caldera in a Densely Populated Area* (Springer, 2022). https://doi.org/10.1007/978-3-642-37060-1
6. Brancaccio, L. et al. Geomorphology and neotectonic evolution of a sector of the tyrrhenian flank of the Southern apennines (region of Naples, Italy). *Z. Geomorph Suppl. Bd.* **82**, 47–58 (1991).
7. Cinque, A., Patacca, E., Scandone, P. & Tozzi, M. Quaternary kinematic evolution of the Southern apennines. Relationships between surface geological features and deep lithospheric structures. *Ann. Geofis.* **36**, 2, 249–259 (1993).
8. Milia, A., Torrente, M. M., Russo, M. & Zuppetta, A. Tectonics and crustal structure of the campania continental margin: relationships with volcanism. *Mineral. Petrol.* **79**, 33–47 (2003).
9. Ortolani, F. & Aprile, F. Nuovi Dati Sulla struttura profonda Della Piana Campana a sud-est Del Fiume Volturno. *Bollettino Della Società Geologica Italiana*. **97** (4), 591–608 (1978).
10. Santangelo, N., Romano, P., Ascione, A. & Ermolli, E. R. Quaternary evolution of the Southern apennines coastal plains: A review. *Geol. Carpath.* **68** (1), 43 (2017).
11. Ippolito, F., Ortolani, F. & Russo, M. Struttura marginale Tirrenica Dell'Appennino Campano: reinterpretazione Di Dati Di Antiche ricerche Di Idrocarburi. *Mem. Soc. Geol. Ital.* **12**, 227–250 (1973). (in Italian with English abstract).
12. Bernasconi, A., Bruni, P., Gorla, L., Principe, C. & Sbrana, A. Preliminary results of deep geothermal exploration in the Somma–vesuvius volcanic area. *Rend. Soc. Geol. Ital.* **4**, 237–240 (1981). (in Italian with English abstract).
13. Balducci, S., Vaselli, M. & Verdini, G. : Exploration well in Ottaviano permit, Italy, trecase 1. European geothermal update 3rd int. Sem., (1983). Munich 29 Nov–Dec., 407–418.
14. Brocchini, D., Principe, C., Castradori, D., Laurenzi, M. A. & Gorla, L. Quaternary evolution of the Southern sector of the campania plain and early Somma–Vesuvius activity: insights from the trecase 1 well. *Mineral. Petrol.* **73**, 67–91 (2001).
15. Servizio Geologico d'Italia. Geological maps of Italy, scale 1:100,000, Sheets 171, 172, 173, 184, 185. (1963–1972). Retrieved from https://sgi.isprambiente.it/geologia100k/

16. Bruno, P. P., Di Fiore, V. & Ventura, G. Seismic study of the '41st parallel'fault system offshore the Campanian–Latial continental margin. *Italy Tectonophysics*. **324** (1–2), 37–55 (2000).
17. Milano, G., Giovambattista, R. & Ventura, G. Seismic activity in the transition zone between Southern and central apennines (Italy): evidences of longitudinal extension inside the Ortona–Roccamonfina tectonic line. *Tectonophysics* **457**, 102–110. https://doi.org/10.1016/J.TECTO.2008.05.034 (2008).
18. Mariani, M. & Prato, R. I Bacini neogenici Del margine Tirrenico: approccio Sismico stratigrafico. *Mem. Soc. Geol. It*. **41**, 519–531 (1988).
19. Torrente, M. M. & Milia, A. Volcanism and faulting of the campania margin (Eastern tyrrhenian Sea, Italy): a three-dimensional visualization of a new volcanic field off Campi flegrei. *Bull. Volcanol.* **75**, 1–13 (2013).
20. Vitale, S. & Ciarcia, S. Tectono-stratigraphic setting of the campania region (southern Italy). *J. Maps*. **14**, 9–21. https://doi.org/10.1080/17445647.2018.1424655 (2018).
21. Del Prete, S., Di Crescenzo, G., Santangelo, N. & Santo, A. Collapse sinkholes in campania (southern Italy): predisposing factors, genetic hypothesis and susceptibility. *Geomorphology* **54**, 259–284 (2010).
22. Celico, P., Civita, M. & Corniello, A. Idrologia del margine nord-orientale della conca campana (Massicci dei Tifatini e del Monte Maggiore). Mem. e Note dell'Istituto di Geologia Applicata dell'Università di Napoli, 13, 1974–1977, p. 29. (1977).
23. Oliveri, D. C. A. & Quagliariello, M. T. Sulla genesi Del Bradisismo Flegreo. *Atti Ass Geofis. Fail.* **18**, 557–594 (1969).
24. De Vivo, B. et al. New constraints on the pyroclastic eruptive history of the Campanian volcanic plain (Italy). *Mineral. Petrol.* **73**, 47–65 (2001).
25. Rolandi, G., Bellucci, F., Heizler, M. T., Belkin, H. E. & De Vivo, B. Tectonic controls on the genesis of ignimbrites from the Campanian volcanic zone, Southern Italy. *Mineral. Petrol.* **79**, 3–31 (2003).
26. Chiesa, S., Cornette, Y. & Gillot, P. Y. and Vezzoli L., - New interpretation of Roccamonfina volcanic history. Abstract, IAVCEI Meeting, Naxos, Sept. 1985. (1985).
27. Di Radicati, F., Di Girolamo, P., Turi, B. & Oddone, M. –40Ar-39Ar e K-Ar dating of K-rich rocks from the Roccamonfina volcano, Roman comagmatic region, Italy. *Geoch Cosmoch Acta*. **52**, 1435–1441 (1988).
28. Gillot, P. Y., Chiesa, S., Pasquare, G. & Vezzoli, L. < 33,000-yr K–Ar dating of the volcano–tectonic Horst of the Isle of Ischia, Gulf of Naples. *Nature* **299** (5880), 242–245 (1982).
29. Rosi, M. & Sbrana, A. Phlegrean fields. Quaderni de La Ricerca scientifica. *CNR Roma*. **114**, 9, 1–175 (1987). Gillot P.Y.
30. Di Girolamo, P., Ghiara, M. R., Lirer, Munno, R., Rolandi, G. & Stanzione, D. Vulcanologia e petrologia dei Campi flegreei. *Bollettino Della Società Geologica Italiana*. **103** (2), 349–413 (1984).
31. Finetti, I. & Morelli, C. Esplorazione sismica a riflessione dei Golfi di Napoli e Pozzuoli, Boll. Geofis. Teor. Appl., 16 (1974), pp. 175–222 (1974).
32. Giaccio, B., Hajdas, I., Isaia, R., Deino, A. & Noma, S. High-precision 14 C and 40Ar/39Ar dating of the Campanian Ignimbrite (Y-5) reconciles the time-scales of climatic-cultural processes at 40 ka. *Sci. Rep.* **7** https://doi.org/10.1038/srep45940 (2017).
33. Deino, A. L., Orsi, G., Piochi, M. & De Vita, S. The age of the Neapolitan yellow tuff caldera-forming eruption (Campi flegrei caldera – Italy) assessed by 40Ar/39Ar dating method. *J. Volcanol Geotherm. Res.* **133**, 157–170 (2004).
34. Matano, F., Sacchi, M., Vigliotti, M. & Ruberti, D. Subsidence trends of volturno river coastal plain (northern campania, southern italy) inferred by sar interferometry data. Geosciences, 8(1), p.8. (2018).
35. Corrado, G., Amodio, S., Aucelli, P. P. C., Pappone, G. & Schiattarella, M. The subsurface geology and landscape evolution of the Volturno coastal plain, Italy: interplay between tectonics and Sea-Level changes during the quaternary. *Water* **12** (12), 3386. https://doi.org/10.3390/w12123386 (2020).
36. Gaudiosi, G., Alessio, G., Luiso, P., Nappi, R. & Ricciolino, P. A critical review of seismotectonic setting of the Campanian Plain (Southern Italy) in GIS environment. In EGU General Assembly Conference Abstracts (p. 12142). (2010).
37. Luiso, P. et al. A multidisciplinary approach to characterize the geometry of active faults: the example of Mt. Massico, Southern Italy). *Geophys. J. Int.* **213**, 1673–1681 (2018).
38. Sheriff, R. E. & Geldart, L. P. *Exploration Seismology* (Cambridge University Press, 1995).
39. Yilmaz, Ö. *Seismic Data Analysis: Processing, Inversion, and Interpretation of Seismic Data* (Society of exploration geophysicists, 2001).
40. Claerbout, J. F. & Doherty, S. M. Downward continuation of moveout-corrected seismograms. *Geophysics* **37** (5), 741–768 (1972).
41. Sopher, D. Converting scanned images of seismic reflection data into SEG-Y format. *Earth Sci. Inf.* **11** (2), 241–255 (2018).
42. Carrozzo, M. T., Luzio, D., Margiotta, C. & Quarta, T. Gravity Anomaly Map of Italy. CNR: Progetto Finalizzato Geodinamica – Sub-project: Modello Strutturale Tridimensionale (in Italian) (1986).
43. AGIP. *Carta Aeromagnetica d'Italia (scala 1:500.000). Att. Min., Direz. Espl. Idrocarburi* (S. Donato Milanese, 1981).
44. Brancaccio, L. et al. Evoluzione Tettonica e geomorfologica Della Piana Del Sele (Campania, Appennino Meridionale): Tectonic and geomorphological evoltion of the Sele Plain (Campania, Southern Apennine). *Geografia Fisica E Dinamica Quaternaria*. **10** (1), 47–55 (1987).
45. Florio, G., Fedi, M., Cella, F. & Rapolla, A. The Campanian plain and phlegrean fields: structural setting from potential field data. *J. Volcanol. Geoth. Res.* **91** (2–4), 361–379 (1999).
46. Amorosi, A., Pacifico, A., Rossi, V. & Ruberti, D. Late quaternary incision and deposition in an active volcanic setting: the Volturno Valley fill, Southern Italy. *Sediment. Geolgy*. **282**, 307–320 (2012).
47. Aiello, G. & Cicchella, A. G. Dati sismostratigrafici Sul margine continentale Della campania Tra Ischia, Capri ed Il bacino Del Volturno (Tirreno meridionale, Italia) in base al processing Sismico ed all'interpretazione geologica Di profili sismici a Riflessione multicanale. *Quad. Di Geofis.*, (149), 1–48. (2018).
48. Cressie, N. A. C. *Statistics for Spatial Data*, John Wiley and Sons, Inc., (900pp). (1991).
49. Tarquini, S., Isola, I., Favalli, M., Battistini, A. & Dotta, G. TINITALY, a digital elevation model of Italy with a 10 meters cell size (Version 1.1). Istituto Nazionale di Geofisica e Vulcanologia (INGV). (2023). https://doi.org/10.13127/tinitaly/1.1
50. Barbieri, M., Di Girolamo, P., Locardi, E., Lombardi, G. & Stanzione, D. Geothermal research in Western Campania (Southern Italy): Stratigraphy of the Parete 2 exploratory well and new data on the volcanic sequence. In International Congress On Thermal Waters, Geothermal Energy And Volcanism In the Mediterranean Area (pp. 100–114). (1976).
51. De Rita, D. & Giordano, G. Volcanological and structural evolution of Roccamonfina volcano (Italy): origin of the summit caldera. *Geol. Soc. Lond. Special Publications*. **110** (1), 209–224 (1996).
52. Fedi, M. & Florio, G. Detection of potential fields source boundaries by enhanced horizontal derivative method. *Geophys. Prospect.* **49** (1), 40–58 (2001).
53. Fedi, M. Multiscale derivative analysis: A new tool to enhance detection of gravity source boundaries at various scales. *Geophys. Res. Lett.* **29** (2), 16–11 (2002).
54. Tavani, S., Cardello, G. L., Vignaroli, G., Balsamo, F., Parente, M., Sabbatino, M.,… Carminati, E. (2021). Segmentation of the Apenninic Margin of the Tyrrhenian Back-Arc Basin Forced by the Subduction of an Inherited Transform System. Tectonics, 40(9), e2021TC006770.
55. Florio, G., Milano, M. & Cella, F. Gravity mapping of basement depth in seismogenic, fault-controlled basins: the case of middle Aterno Valley (Central Italy). *Tectonophysics* **817**, 229044 (2021).
56. Grauch, V. J. S. & Cordell, L. Limitations of determining density or magnetic boundaries from the horizontal gradient of gravity or pseudogravity data. *Geophysics* **52** (1), 118–121 (1987).

57. Cinque, A., Ascione, A. & Caiazzo, C. Distribuzione Spaziotemporale e caratterizzazione Della fagliazione quaternaria in Appennino meridionale, Le Ricerche Del GNDT Nel Campo Della Pericolosità Sismica, in (eds, F.,, C. &, A.) 203–218, CNR – Gruppo Nazionale per la Difesa dai Terremoti – Rome (2000). (in Italian).
58. Milia, A. & Torrente, M. M. Tectono-stratigraphic signature of a rapid multistage subsiding rift basin in the Tyrrhenian-Apennine hinge zone (Italy): A possible interaction of upper plate with subducting slab. *J. Geodyn.* **86**, 42–60 (2015).
59. Turco, E., Schettino, A., Pierantoni, P. P. & Santarelli, G. The pleistocene extension of the campania plain in the framework of the Southern tyrrhenian tectonic evolution: morphotectonic analysis, kinematic model and implications for volcanism. In Developments in Volcanology (Vol. 9, 27–51). Elsevier. (2006).
60. ISPRA. Geological maps of Italy, scale 1:50,000, Sheets 416, 417, 418, 429, 430, 431, 446, 447, 448. (2017). Retrieved from www.isprambiente.gov.it/Media/carg/
61. Buffardi, C., Barbato, R., Vigliotti, M., Mandolini, A. & Ruberti, D. The holocene evolution of the Volturno coastal plain (Northern Campania, Southern Italy): implications for the Understanding of subsidence patterns. *Water* **13** (19), 2692 (2021).
62. ISIDe Working Group Italian seismological instrumental and parametric database (ISIDe) (Version 1). *Istituto Naz. Di Geofis. E Vulcanologia (INGV)*. https://doi.org/10.13127/ISIDE (2007).
63. Rovida, A. et al. Catalogo Parametrico dei Terremoti Italiani (CPTI15), versione 4.0 [Data set]. Istituto Nazionale di Geofisica e Vulcanologia (INGV). https://doi.org/10.13127/cpti/cpti15.4. (2022).
64. Acocella, V., Salvini, F., Funiciello, R. & Faccenna, C. The role of transfer structures on volcanic activity at Campi flegrei (Southern Italy). *J. Volcanol. Geoth. Res.* **91**, 123–139. https://doi.org/10.1016/S0377-0273(99)00032-3 (1999).
65. D'Antonio, M. et al. The present state of the magmatic system of the Campi Flegrei caldera based on a reconstruction of its behavior in the past 12 ka. *J. Volcanol Geotherm. Res.* **91**, 247–268 (1999).
66. Bruno, P. P. G., Rapolla, A. & Di Fiore, V. Structural setting of the Bay of Naples (Italy) seismic reflection data: implications for Campanian volcanism. *Tectonophysics* **372**, 192–213 (2003).
67. Bruno, P. P. G. Structure and evolution of the Bay of pozzuoli (Italy) by marine seismic data. *Bull. Volcanol.* **66**, 342–355. https://doi.org/10.1016/s0040-1951(03)0 (2004).
68. Judenherc, S. & Zollo, A. The Bay of Naples (southern Italy): constraints on the volcanic structures inferred from a dense seismic survey. *J. Geophys. Research: Solid Earth.* **109**, B10 (2004).
69. Piochi, M., Bruno, P. P. & De Astis, G. Relative roles of rifting tectonics and magma ascent processes: inferences from geophysical, structural, volcanological, and geochemical data for the Neapolitan volcanic region (southern Italy). *Geochemistry Geophys. Geosystems*, **6**(7). (2005).
70. Milia, A. & Torrente, M. M. Tectonics and stratigraphic architecture of a peri-Tyrrhenian half-graben (Bay of Naples, Italy). *Tectonophysics* **315** (1–4), 301–318 (1999).
71. Acocella, V. & Funiciello, R. Transverse systems along the extensional tyrrhenian margin of central Italy and their influence on volcanism. *Tectonics*, **25**(2). (2006).
72. Mariucci, M., Pierdominici, S. & Montone, P. Scientific drilling in a central Italian volcanic district. *Sci. Drill.* **5**, 38–40. https://doi.org/10.2204/IODP.SD.5.04.2007 (2007).
73. Liotta, D. & Brogi, A. Pliocene-Quaternary fault kinematics in the Larderello geothermal area (Italy): insights for the interpretation of the present stress field. *Geothermics* **83**, 101714 (2020).
74. Brogi, A., Liotta, D., Capezzuoli, E., Matera, P. F., Kele, S., Soligo, M., … Huntington,K. W. (2020). Travertine deposits constraining transfer zone neotectonics in geothermal areas: An example from the inner Northern Apennines (Bagno Vignoni-Val d'Orcia area,Italy). Geothermics, 85, 101763.
75. Cinque, A. et al. Ground movements and sea level changes in urban areas: 5000 years of geological and archaeological record from Naples (Southern Italy). *Quatern. Int.* **232** (1–2), 45–55 (2011).

Acknowledgements
We gratefully acknowledge the Landmark Grant Program, sponsored by Halliburton Software and Services, for supporting the University of Naples Federico II. We also thank dGB Earth Science for providing an academic license for OpendTect Pro software. Special thanks go to Dario Cuollo and Raffaele Moio, geology students at the University of Naples Federico II, for their contributions to the preliminary seismic data interpretation as part of their bachelor's (R.M.) and master's (D.C.) theses under the supervision of Pier Paolo G. Bruno.

Author contributions
P.P.G. Bruno processed and interpreted the seismic data, with interpretative input from M.L. Putignano. G. Florio and F. Cella processed and analyzed the gravity and magnetic data. P.P.G. Bruno was the primary author of the manuscript, with G. Florio and F. Cella contributing to sections on potential field data and comparative analysis. All authors participated in the finalization of the manuscript.

Declarations

Competing interests
The authors declare no competing interests.

Additional information
Correspondence and requests for materials should be addressed to P.P.G.B.